



Local Adaptation of Bitter Taste and Ecological Speciation in a Wild Mammal

Hengwu Jiao ^{†,1} Qian Wang^{†,1} Bing-Jun Wang,¹ Kexin Li,^{2,3} Matěj Lövy,⁴ Eviatar Nevo,² Qiyang Li,¹ Wenchuan Su,¹ Peihua Jiang,⁵ and Huabin Zhao ^{*,1,6}

¹Department of Ecology, Tibetan Centre for Ecology and Conservation at Wuhan University—Tibet University, Hubei Key Laboratory of Cell Homeostasis, College of Life Sciences, Wuhan University, Wuhan, China

²Institute of Evolution, University of Haifa, Haifa, Israel

³State Key Laboratory of Grassland Agro-Ecosystem, Institute of Innovation Ecology, Lanzhou University, Lanzhou, China

⁴Department of Zoology, Faculty of Science, University of South Bohemia, České Budějovice, Czech Republic

⁵Monell Chemical Senses Center, Philadelphia, PA, USA

⁶Research Center for Ecology, College of Science, Tibet University, Lhasa, China

[†]These authors contributed equally to this work.

*Corresponding author: E-mail: huabinzhao@whu.edu.cn.

Associate editor: Jianzhi Zhang

Abstract

Sensory systems are attractive evolutionary models to address how organisms adapt to local environments that can cause ecological speciation. However, tests of these evolutionary models have focused on visual, auditory, and olfactory senses. Here, we show local adaptation of bitter taste receptor genes in two neighboring populations of a wild mammal—the blind mole rat *Spalax galili*—that show ecological speciation in divergent soil environments. We found that basalt-type bitter receptors showed higher response intensity and sensitivity compared with chalk-type ones using both genetic and cell-based functional analyses. Such functional changes could help animals adapted to basalt soil select plants with less bitterness from diverse local foods, whereas a weaker reception to bitter taste may allow consumption of a greater range of plants for animals inhabiting chalk soil with a scarcity of food supply. Our study shows divergent selection on food resources through local adaptation of bitter receptors, and suggests that taste plays an important yet underappreciated role in speciation.

Key words: local adaptation, bitter taste, ecological speciation, functional assay.

Introduction

Understanding the link between speciation and natural selection has been a central topic in the field of evolutionary biology since Darwin (Darwin 1859). Ecological speciation is a model of speciation that occurs as a by-product of natural selection (Rundle and Nosil 2005; Schluter 2009; Schluter and Conte 2009), whereby divergent selection drives local adaptation to ecologically different environments, eventually leading to reproductive isolation between populations (Mayr 1947; Schluter 2001). Local environments can differ in a variety of biotic and abiotic factors, including food resources, climate, temperature, habitat, and interaction with other species such as predators and pollinators (Rundle and Nosil 2005; Sobel et al. 2010). Sensory systems are attractive evolutionary models to address how natural selection shapes local adaptation that can cause ecological speciation, because they could connect external environmental signals with internal physiological responses. However, although visual, auditory, and olfactory senses were suggested to be involved in

numerous examples of ecological speciation (Kingston and Rossiter 2004; Seehausen et al. 2008; Keeseey et al. 2020), the role of other sensory modalities, for example taste, has been underappreciated in speciation.

Two neighboring populations of a wild mammal, the blind mole rat *Spalax galili*, in northern Israel living in two contrasting soil environments—chalk and basalt—have been identified as a unique model of ecological sympatric speciation (Hadid et al. 2013; Li et al. 2015, 2016; Lövy et al. 2015, 2017) (fig. 1). One of the most significant differences between these soils is food resource. In general, basalt soil offers higher diversity and abundance of food resources than chalk soil (Lövy et al. 2015, 2017) (fig. 1). This is likely caused by a higher abundance of *Sarcopoterium spinosum* bushes in chalk soil (fig. 1), which effectively outcompete other herbaceous vegetation including plants with various underground storage organs such as geophytes—the staple food of mole rats (Mohammad and Alseekh 2013). It is thus suggested that mole rats living in chalk soil are exposed to more stressful conditions in terms of food supply.

© The Author(s) 2021. Published by Oxford University Press on behalf of the Society for Molecular Biology and Evolution.

This is an Open Access article distributed under the terms of the Creative Commons Attribution Non-Commercial License (<http://creativecommons.org/licenses/by-nc/4.0/>), which permits non-commercial re-use, distribution, and reproduction in any medium, provided the original work is properly cited. For commercial re-use, please contact journals.permissions@oup.com

Open Access

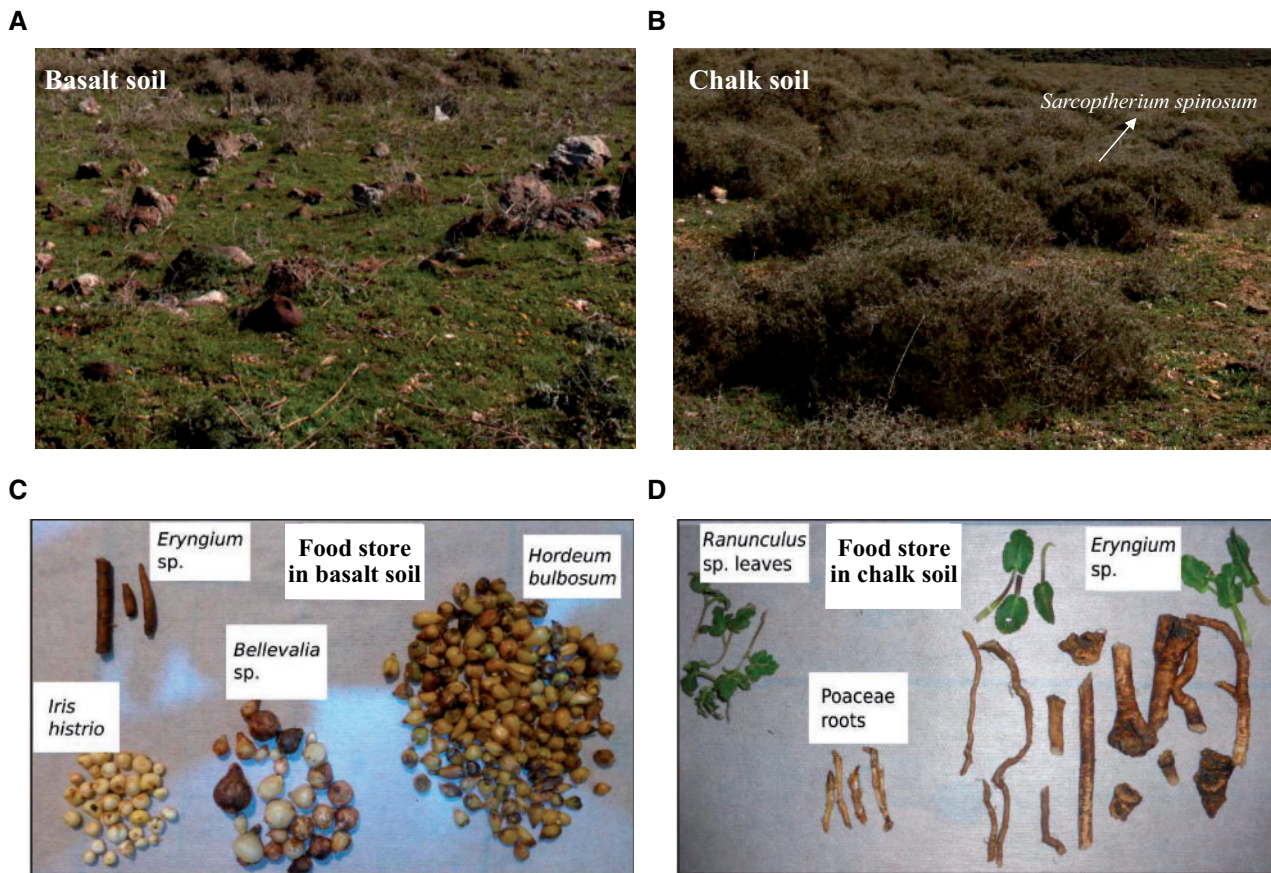


FIG. 1. Vegetation characteristics and food stores in basalt and chalk soils. Distinct patterns of plant diversity and food stores were observed in basalt soil (A and C) and chalk soil (B and D). The chalk soil is covered by the highly abundant *Sarcopoterium spinosum* bushes. Pictures of the studied microsites were provided by Matěj Lövy.

Therefore, food could be one of the important agents of divergent selection that subsequently promotes local adaptation to the ancestral chalk and derived basalt soil environments (Weinstein et al. 2006; Hadid et al. 2013; Li et al. 2015). In an earlier study (Li et al. 2015), we detected genetic divergence of several olfactory and taste receptors between the two neighboring populations, indicating that sensory systems may be involved in ecological speciation of the blind mole rat, although functional divergence of these receptors between populations remains unknown.

In this study, we focused on the bitter taste receptors (Tas2rs) that can detect potentially toxic compounds in environments, and thus determine food selection. We hypothesized that functional divergence of Tas2rs may drive local adaptation to different food resources. Indeed, functional diversity of TAS2R1, TAS2R4, and TAS2R16 was detected in primates with different diets; such diversity could help different primate species to adapt to the food items they eat (Imai et al. 2012; Tsutsui et al. 2016). Moreover, functional differentiation of Tas2r20 receptor among giant panda populations was found to be associated with different contents of quercitrin in bamboo leaves (Hu et al. 2020). Local adaptation to different food resources may eventually lead to habitat-based assortative mating, which is considered to be a strong driving

force in ecological speciation (Berner and Thibert-Plante 2015; Lövy et al. 2017; Kopp et al. 2018).

Here, we examine all *Tas2r* genes that are putatively functional in the two divergent soil populations of *S. galili*, including sequences that were previously reported as well as those that are newly generated in this study. We performed population genetic analysis, including F_{ST} measurement and haplotype phasing, to examine whether divergent selection plays a major role in the evolution of these putatively functional *Tas2rs* between the two populations. More importantly, we used cell-based functional assays of six differentiated *Tas2rs* to test for functional divergence between these two populations.

Results

Tas2r Identification and Gene Sequencing

Tas2rs are genes without introns, and have an average length of ~900 nucleotides. Using a method previously described (Jiao et al. 2018), we identified 32 intact *Tas2rs* from the genome sequence of the blind mole rat. We then constructed a gene tree using IQ-TREE (Nguyen et al. 2015), based on the alignment of the 32 *Tas2rs* identified here and 288 intact rodent *Tas2rs* obtained from a previous study (Hayakawa et al. 2014). We found that 20 of the 32 *Tas2rs* have

orthologous genes in other rodents, whereas the other 12 are species-specific (supplementary fig. S1, Supplementary Material online). In this study, we successfully amplified and sequenced the complete regions of 12 *Tas2rs* in 16 individuals from the basalt environment and 13 from the chalk environment. Combined with the other 20 *Tas2rs* previously sequenced in the same individuals (Li et al. 2015), our data set includes the sequences of all 32 intact *Tas2rs* in *S. galili*.

Genetic Differentiation of *Tas2rs* in the Two Populations

To examine the population genetic differentiation of these *Tas2rs*, pairwise F_{ST} values between the two populations were measured for each *Tas2r* gene using DnaSP (Librado and Rozas 2009). We found that ten *Tas2rs* are significantly differentiated between the chalk and basalt populations ($P < 0.05$, after false discovery rate [FDR] adjustment; supplementary table S1, Supplementary Material online). To further test whether *Tas2rs* genes evolved under natural selection, we utilized 18 randomly selected noncoding regions from the genome, which were previously sequenced in the same 29 individuals (Li et al. 2015). Only one of these regions showed significant genetic differentiation between the two populations (Li et al. 2015). Distinct distributions of F_{ST} values for *Tas2r* genes and noncoding regions were clearly observed (fig.

2A). Furthermore, the frequency of significantly differentiated loci is statistically higher in *Tas2rs* (10/32 = 31.25%) than in noncoding regions (1/18 = 5.56%) ($P = 0.041$, two-tailed Fisher's exact test), suggesting that natural selection, rather than neutral processes, may have shaped the evolution of *Tas2rs* between the two populations.

Using the PHASE program (Stephens and Donnelly 2003), we inferred the nucleotide haplotypes for each *Tas2r* gene. A total of 214 nucleotide haplotypes were identified among the 32 *Tas2rs* (supplementary table S2, Supplementary Material online). In order to detect the haplotype differences that may be associated with functional differences, we further obtained the protein haplotypes for each *Tas2r* gene and compared the frequencies of each protein haplotype in the basalt population with those in the chalk population using Fisher's exact test (supplementary tables S3 and S4, Supplementary Material online). Our results showed that there are six *Tas2r* genes (*Sg_Tas2r118*, *Sg_Tas2r119*, *Sg_Tas2r134*, *Sg_Tas2r137*, *Sg_Tas2r143*, and *Sg_Tas2r582a*) that have at least one significantly differentiated protein haplotype (fig. 2B–D and supplementary fig. S2, Supplementary Material online). For example, *Sg_Tas2r118* has seven protein haplotypes (supplementary fig. S3, Supplementary Material online), of which six were found in the basalt population and five were found in the chalk population (fig. 2B). The frequency

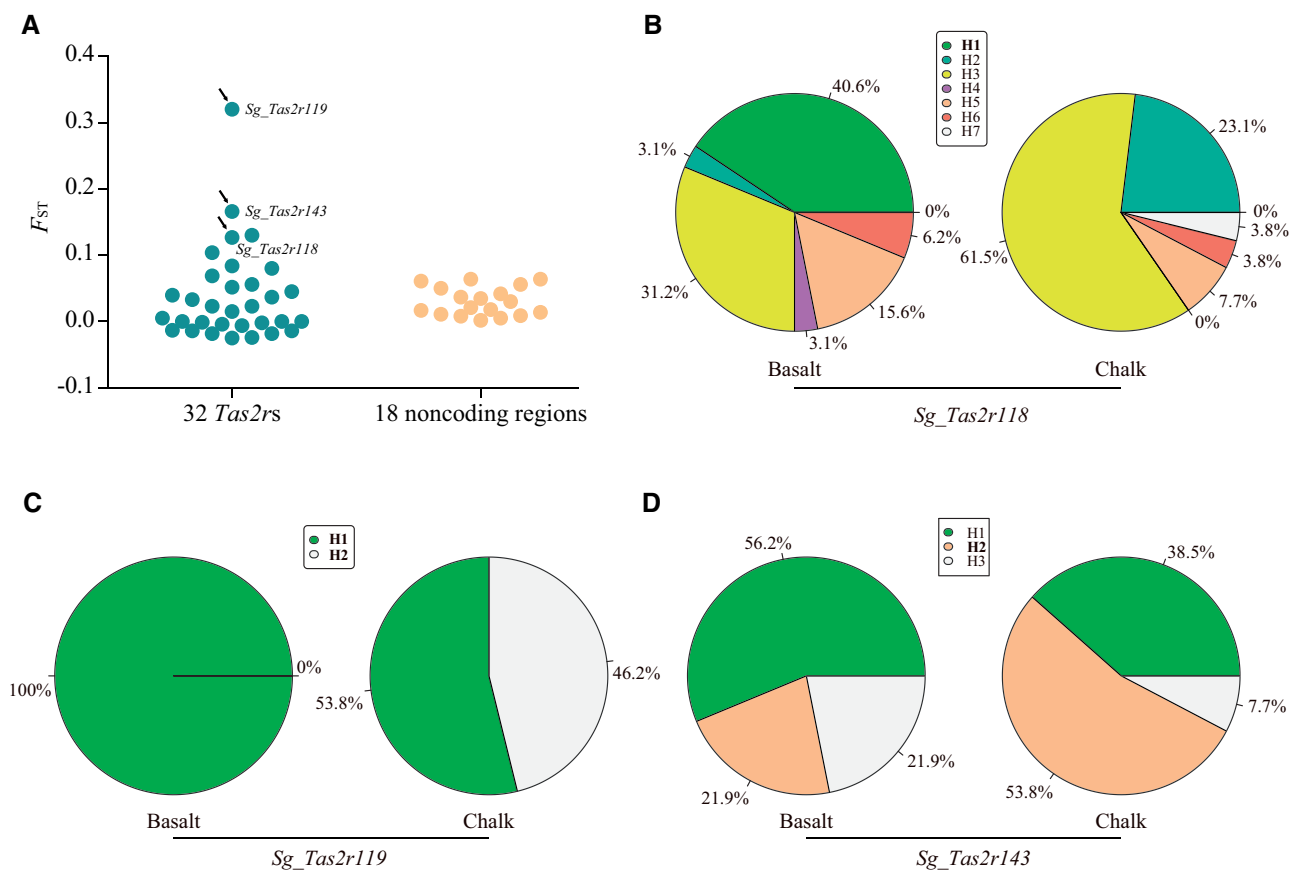


Fig. 2. Population genetic analysis of *Spalax Tas2r* genes. (A) The distribution of F_{ST} value for 32 *Tas2r* genes and 18 noncoding regions. The arrow indicates that these *Tas2rs* exhibited functional divergence between the two populations. (B–D) Protein haplotype distribution of *Sg_Tas2r118* (B), *Sg_Tas2r119* (C), and *Sg_Tas2r143* (D). For each gene, different protein haplotypes are marked with various colors. The percentages of each haplotype in each population are also shown. Significantly differentiated protein haplotypes were shown in bold.

of protein haplotype Sg_Tas2r118 (H1) is significantly higher in the basalt population ($13/32 = 40.6\%$) than in the chalk population ($0/26 = 0\%$) ($P = 0.001$, after FDR adjustment, two-tailed Fisher's exact test, [fig. 2B](#) and [supplementary table S4, Supplementary Material](#) online). Sg_Tas2r119 has two protein haplotypes; Sg_Tas2r119 (H1) is shared between the two populations, whereas Sg_Tas2r119 (H2) is unique to the chalk population, and occurs at a high frequency ($12/26 = 46.2\%$) ([fig. 2C](#) and [supplementary table S4, Supplementary Material](#) online). Sg_Tas2r143 has three protein haplotypes, all of which are shared between the two populations ([fig. 2D](#)). However, the frequency of the protein haplotype Sg_Tas2r143 (H2) is statistically lower in the basalt population ($7/32 = 21.9\%$) than in the chalk population ($14/26 = 53.8\%$) ($P = 0.045$, after FDR adjustment, two-tailed Fisher's exact test, [fig. 2D](#) and [supplementary table S4, Supplementary Material](#) online). Similar results can also be found in the other three differentiated *Tas2r* genes, including Sg_Tas2r134, Sg_Tas2r137, and Sg_Tas2r582a ([supplementary fig. S2, Supplementary Material](#) online). In addition, these six above-mentioned *Tas2rs* were also significantly differentiated between the two populations in the F_{ST} analysis ([supplementary table S1, Supplementary Material](#) online). This finding strongly suggests that these six *Tas2r* genes are under divergent selection and may exhibit functional divergence between the two populations.

Functional Divergence of *Tas2rs* in the Two Populations

Of the six *Tas2rs* that were significantly differentiated between the two populations based on the F_{ST} and protein haplotype analysis ([fig. 2](#) and [supplementary fig. S2, Supplementary Material](#) online), significantly differentiated haplotypes of four *Tas2rs* (Sg_Tas2r119, Sg_Tas2r134, Sg_Tas2r137, and Sg_Tas2r143) have only one amino acid change, and that of the remaining two *Tas2rs* (Sg_Tas2r118 and Sg_Tas2r582a) have multiple amino acid changes ([fig. 3A](#) and [supplementary fig. S2, Supplementary Material](#) online). It is worth noting that these amino acid changes are not fixed in either population because the two populations separated very recently (Li et al. 2015). Based on the frequencies of protein haplotypes in these *Tas2rs* ([fig. 2B–D](#) and [supplementary fig. S2, Supplementary Material](#) online), we selected two protein haplotypes for each *Tas2r*, one from the basalt population and the other from the chalk population, for cell-based functional assays. For example, for Sg_Tas2r118, Sg_Tas2r118 (H1), and Sg_Tas2r118 (H3) were selected, hereafter renamed as Sg_Tas2r118B (B denotes Basalt) and Sg_Tas2r118C (C denotes Chalk) ([fig. 3A](#)). A similar renaming was applied to each selected protein haplotype for the other five *Tas2rs*, where each haplotype is appended with a B or C for basalt or chalk, respectively ([fig. 3A](#) and [supplementary fig. S2, Supplementary Material](#) online). We examined the responses of the two selected protein haplotypes of each of the six *Tas2rs* to 20 bitter compounds with distinct chemical structures ([supplementary table S5, Supplementary Material](#) online). Our screening results showed that although no functional divergence was found between the two selected

protein haplotypes of Sg_Tas2r134, Sg_Tas2r137, and Sg_Tas2r582a ([supplementary table S6, Supplementary Material](#) online), the two protein haplotypes of the remaining three *Tas2rs* (Sg_Tas2r118, Sg_Tas2r119, and Sg_Tas2r143) exhibited clear difference on the responses to two to five bitter compounds ([fig. 3](#)). We confirmed that the functional divergence was not due to the difference of *Tas2r* haplotype expression levels in HEK293 cells by immunofluorescence assay ([supplementary fig. S4, Supplementary Material](#) online). The bitter receptor Sg_Tas2r118 can be activated by five natural bitter compounds, including four beta-glucopyranosides (amygdalin, helicin, salicin, and arbutin) and one sesquiterpenoid (picrotoxinin) ([fig. 3B](#)). Interestingly, we found that the responsiveness of the protein haplotype Sg_Tas2r118B to each of the five compounds is significantly higher than that of Sg_Tas2r118C (one-way ANOVA, Tukey test for multiple comparisons) ([fig. 3B](#)). Furthermore, we obtained the dose–response curves for all five identified compounds ([fig. 3B](#)). Our results showed that Sg_Tas2r118B appears to be more sensitive than Sg_Tas2r118C to each of the five compounds, although the EC50 value cannot be accurately measured in this study owing to the toxicity of these bitter compounds at high concentration in vitro. We also found that Sg_Tas2r119 recognized two compounds, including one natural (camphor) and one synthetic (phenanthroline) ([fig. 3C](#)). Moreover, Sg_Tas2r143 recognized three bitter compounds, including two natural (amygdalin and salicin) and one synthetic (diphenidol) ([fig. 3D](#)). Similarly, the responsiveness of the protein haplotype Sg_Tas2r119B to each ligand is significantly higher than that of the protein haplotype Sg_Tas2r119C (one-way ANOVA, Tukey test for multiple comparisons) ([fig. 3C](#)). Based on the dose–response curves, Sg_Tas2r119B appears to be more sensitive than Sg_Tas2r119C to the two agonists ([fig. 3C](#)). These trends hold true for Sg_Tas2r143 ([fig. 3D](#)). Thus, our findings clearly show that the basalt-type haplotype for each of the three *Tas2rs* has a greater response intensity and sensitivity than the chalk-type haplotype.

Identification of Genetic Changes Responsible for Functional Divergence of Sg_Tas2r118 between the Two Populations

Given that there is only one amino acid difference between the two selected protein haplotypes of Sg_Tas2r119 and Sg_Tas2r143 ([fig. 3A](#)), we reasoned that K121R and D212N are exclusively responsible for the functional divergence of Sg_Tas2r119 and Sg_Tas2r143, respectively ([fig. 3C and D](#)). However, the specific residues that determine functional divergence of Sg_Tas2r118 between the two populations are still unclear, because five amino acids are different between the protein haplotypes Sg_Tas2r118B and Sg_Tas2r118C ([fig. 3A](#)). To assess the functional consequences of these five sites, we performed site-directed mutagenesis to generate five mutant receptors (S173F, M186V, S238F, I249F, and T267M) by replacing each of the five amino acids of protein haplotype Sg_Tas2r118B with that of Sg_Tas2r118C. For example, we mutated the amino acid S173 of Sg_Tas2r118B to F (phenylalanine) to generate the mutant receptor S173F. HEK293 cells

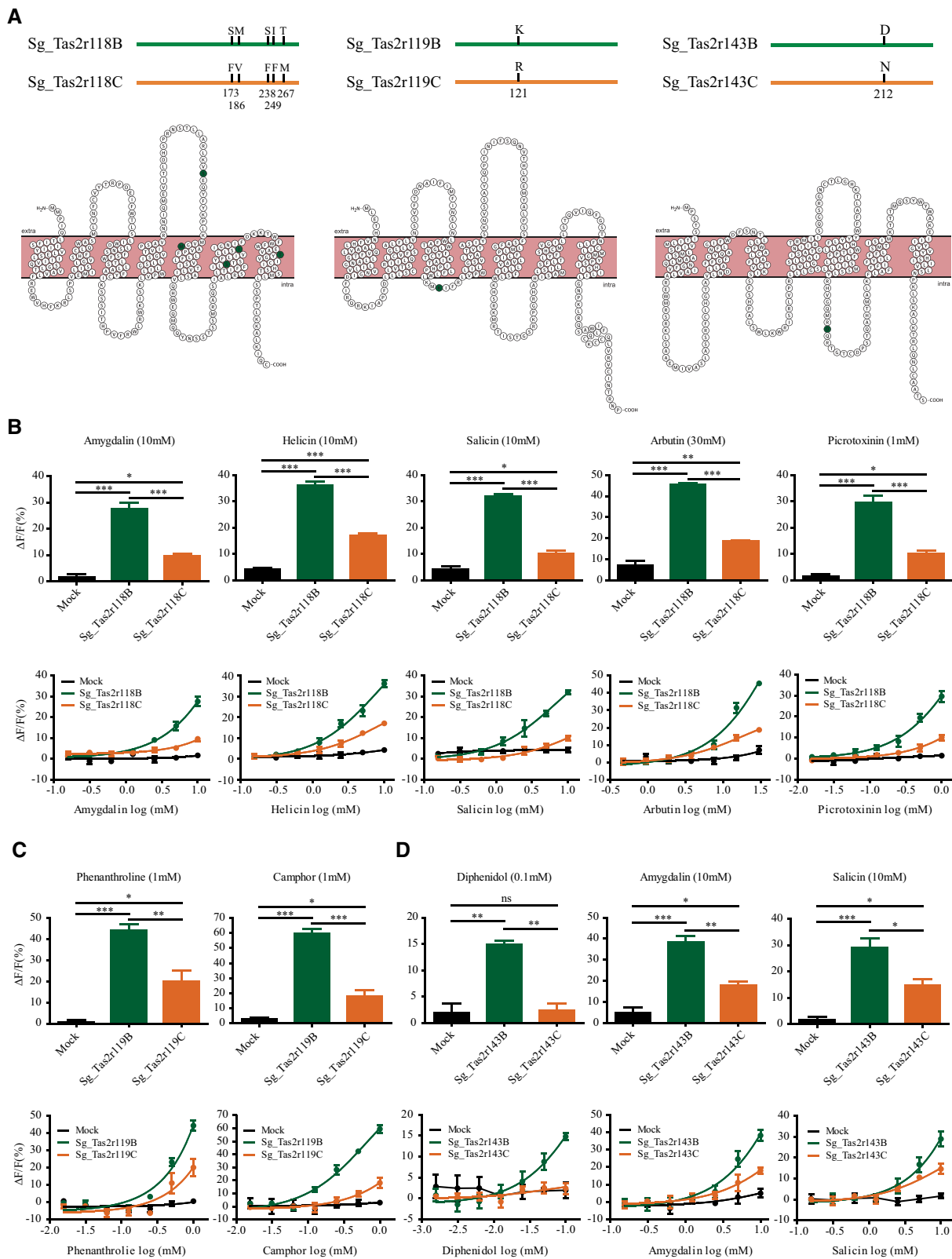


Fig. 3. Functional divergence between basalt-type and chalk-type protein haplotypes of three *Tas2r* genes. (A) Basalt-type protein haplotypes of *Sg_Tas2r118*, *Sg_Tas2r119*, and *Sg_Tas2r143*. The amino acid difference between basalt-predominant and chalk-predominant protein haplotypes is indicated. Snake plot of each *Tas2r* was generated based on the sequence of basalt-type protein haplotype. (B) Functional divergence between *Sg_Tas2r118B* and *Sg_Tas2r118C* to four beta-glucopyranosides (amygdalin, helicin, salicin, and arbutin) and one sesquiterpenoid (picrotoxinin). (C) Functional divergence between *Sg_Tas2r119B* and *Sg_Tas2r119C* to phenanthroline and camphor. (D) Functional divergence between *Sg_Tas2r143B* and *Sg_Tas2r143C* to diphenidol, amygdalin, and salicin. All bar graphs and dose-dependent curves were generated with GRAPHPAD PRISM 5. Analysis of variance with Tukey's multiple comparisons test was used for statistical analysis (* $P < 0.05$, ** $P < 0.01$, *** $P < 0.001$).

expressing these mutant receptors along with $G\alpha_{16}$ -gust44 were then assayed for their responses to the five identified agonists. We assessed the expression levels of five *Tas2r* mutants in HEK293 cells by immunofluorescence assay and found similar expression levels (14.8–20.7%) for different *Tas2r* mutants (supplementary fig. S4, Supplementary Material online). The responsiveness of these mutant receptors to agonists was either similar or significantly reduced when compared with that of *Sg_Tas2r118B* (fig. 4 and supplementary table S7, Supplementary Material online). For example, compared with the background *Sg_Tas2r118B*, the mutant receptor *S238F* showed a similar response to amygdalin (fig. 4A and supplementary table S7, Supplementary Material online). The other four mutant receptors showed significantly reduced responses, similar to the response of *Sg_Tas2r118C* to amygdalin (fig. 4A and supplementary table S7, Supplementary Material online). The dose–response curves further confirm that both *Sg_Tas2r118B* and *S238F* showed similar levels of sensitivity, whereas *Sg_Tas2r118C* and the other four mutant receptors showed similar levels of sensitivity (fig. 4B). These findings suggest that the difference in response of *Sg_Tas2r118B* and *Sg_Tas2r118C* to amygdalin is likely caused by the other four amino acid replacements, rather than *S238F*. Such general pattern was also observed in the other three beta-glucopyranosides (fig. 4), indicative of the obvious effects of those four amino acid replacements (*S173F*, *M186V*, *I249F*, and *T278M*) on the recognition of beta-glucopyranosides. Nonetheless, we noticed that *Sg_Tas2r118B* and its mutant receptor *S238F* showed distinct levels of sensitivity to salicin (fig. 4F), suggesting that the replacement *S238F* may also be involved in salicin binding and contribute to functional divergence between *Sg_Tas2r118B* and *Sg_Tas2r118C* to salicin. As for the non-glucopyranoside agonist picrotoxinin, all five mutant receptors showed significantly reduced responses when compared with *Sg_Tas2r118B* (fig. 4I and supplementary table S7, Supplementary Material online), or similar responses when compared with *Sg_Tas2r118C* (fig. 4I and supplementary table S7, Supplementary Material online). The dose–response curves showed that *Sg_Tas2r118B* is the most sensitive among all assayed receptors, and that five mutant receptors and *Sg_Tas2r118C* exhibit similar degrees of sensitivity (fig. 4J), indicating that all five amino acid replacements are likely to result in functional divergence between *Sg_Tas2r118B* and *Sg_Tas2r118C* to picrotoxinin.

We also performed structure modeling and molecular docking for each haplotype of the three *Tas2rs* to validate the effects of amino acid variants on protein–ligand interaction (supplementary fig. S5, Supplementary Material online). Among those variants examined in this study, only one amino acid, *F249* of *Sg_Tas2r118C*, was predicted to be directly involved in the interaction with helicin, salicin, and arbutin (supplementary fig. S5, Supplementary Material online). Therefore, our structure–function analysis confirms an impact of the replacement *I249F* of *Sg_Tas2r118* on ligand recognition, and suggests that other amino acid variants may also be involved in other aspects of receptor activation, such

as signal transduction and changes in the stability of protein conformation (Singh et al. 2011; Thomas et al. 2017).

Discussion

In this study, we performed population genetic analysis and functional characterization of *Tas2rs* between the two neighboring populations of blind mole rats inhabiting divergent soil conditions. We found that ten of 32 *Tas2rs* show significant differentiation between the two populations based on the F_{ST} measurements. Of these differentiated *Tas2rs*, six were also identified by protein haplotype analysis, indicating that natural selection shapes their genetic divergence. Cell-based functional assays of six *Tas2rs* further confirmed the functional divergence between the basalt-predominated protein haplotype and the chalk-predominated protein haplotype.

The genetic divergence of bitter taste receptors between the two different soil populations has been reported previously by sequencing 20 *Tas2rs* (Li et al. 2015). Here, we sequenced the remaining 12 *Tas2rs* in the same individuals, generating a full data set that includes all putatively functional *Tas2rs*. Ten of the 32 *Tas2rs* were identified as significantly differentiated loci, eight whose orthologs have been detected in other rodent species and two that are species-specific. A similar pattern was also observed in two other chemosensory gene families: olfactory receptor genes and vomeronasal receptor genes (Li et al. 2015; Jiao et al. 2019). This is consistent with rapid evolution of chemosensory receptors that directly respond to new environments (Niimura and Nei 2006; McBride 2007; Brand et al. 2015). However, the significant population differentiation indicated by high F_{ST} values could have resulted from the different frequencies of either non-synonymous or synonymous variations between populations. Although the former are responsible for functional variations, the latter are less important in protein function because they do not lead to amino acid changes. We therefore compared the frequencies of protein haplotypes between the two populations. The protein haplotype was inferred by merging the nucleotide haplotypes with synonymous variations. We identified six *Tas2rs* with at least one significantly differentiated protein haplotype. Interestingly, these six *Tas2rs* can also be identified by F_{ST} analysis, suggesting that population differentiation of these *Tas2rs* were mainly determined by different frequencies of nonsynonymous variations. In contrast, different frequencies of synonymous variations in the other four *Tas2rs* that led to significant population differentiation were identified by F_{ST} analysis but not the protein haplotype analysis. Such remarkable genetic differentiations of bitter taste receptors were also observed in subspecies of chimpanzees (Sugawara et al. 2011; Hayakawa et al. 2012).

Our functional assays demonstrated that functional divergence appears to be present between the basalt-type and chalk-type protein haplotypes of three *Tas2rs* (*Sg_Tas2r118*, *Sg_Tas2r119*, and *Sg_Tas2r143*). In general, the basalt-type protein haplotype of each gene is more sensitive than the chalk-type protein haplotype to agonists. It appears that *K121R* leads to functional divergence of *Sg_Tas2r119*, owing to only one amino acid change between the two protein

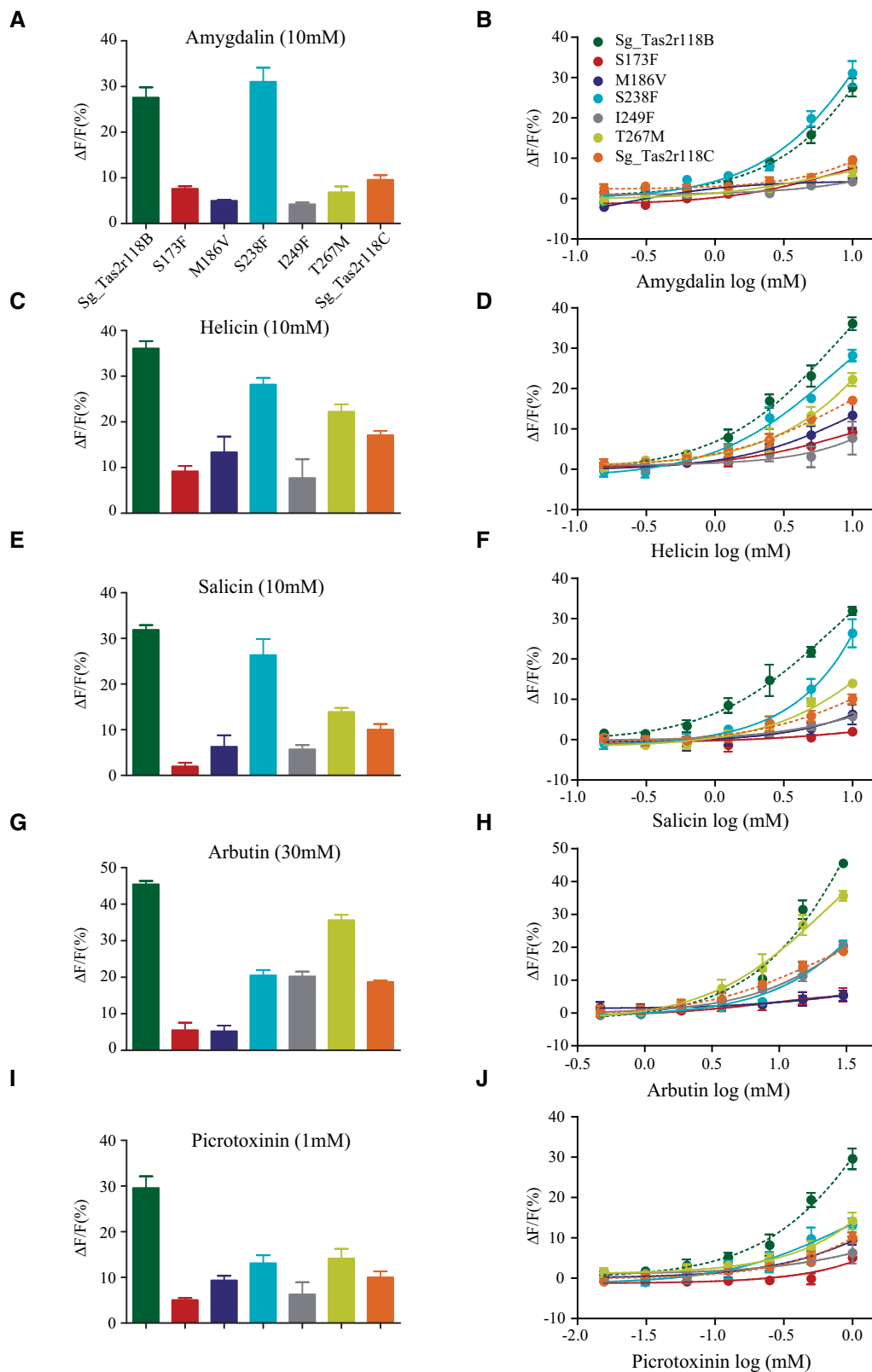


FIG. 4. Identification of key residues that were responsible for the functional divergence of Sg_Tas2r118B and Sg_Tas2r118C. Five mutant receptors were generated using site-directed mutagenesis, and their responses to five agonists were measured. (A, C, E, G, and I) Quantitative analysis of responses of mutant receptors to amygdalin (10 mM), helicin (10 mM), salicin (10 mM), arbutin (30 mM), and picROTOXININ (1 mM), respectively. See the statistical comparisons in [supplementary table S7, Supplementary Material](#) online. (B, D, F, H, and J) Dose-dependent responses of mutant receptors to amygdalin, helicin, salicin, arbutin, and picROTOXININ, respectively. Sg_Tas2r118B and Sg_Tas2r118C (dashed lines) are also included for comparison. Different receptors are indicated by various colors.

haplotypes, whereas D212N accounts for functional divergence of Sg_Tas2r143. By assaying the mutant receptors of Sg_Tas2r118, we found that all five amino acid replacements can affect ligand sensitivity, with the exception of S238F, which is less important in affecting amygdalin binding. These findings suggest that these five amino acids are involved in the recognition of both types of chemical compounds with distinct structures: beta-glucopyranosides (amygdalin, helicin, salicin, and arbutin) and sesquiterpenoids (picrotoxinin). Interestingly, mutations in three of these five amino acid positions in human TAS2R16 (ortholog to Sg_Tas2r118) have been associated with interaction with salicin, thus paralleling our study (Thomas et al. 2017).

Blind mole rats are herbivorous; their diet consists of plants with underground storage organs, such as bulbs, corms, and roots. The bitter taste mediated by Tas2rs has been considered to play an important role for the survival of animals, especially for herbivores and insectivores (Li and Zhang 2014; Wang and Zhao 2015). However, we observed a significantly lower intensity and sensitivity of bitter taste receptors to bitter compounds in the ancestral chalk population compared with the derived basalt population (Weinstein et al. 2006; Li et al. 2015). We used codeml in PAML 4 (Yang 2007) to infer the ancestral states of three functionally divergent Tas2rs at the ancestral node of the two populations (supplementary fig. S6, Supplementary Material online). Our results showed that the basalt-type haplotype is derived, suggesting that positive selection may promote the functional divergence of Tas2rs. These findings indicate that the bitter taste is dull in mole rats inhabiting the ancestral chalk soil environment, and then becomes sensitive in individuals adapted to basalt soils. Moreover, most of the bitter compounds used in this study are common in plants. For example, beta-glucopyranosides and camphor can be found in two plant species (*Ranunculus asiaticus* and *Eryngium creticum*) growing in both soils (Toki et al. 1996; Lövy et al. 2015; Kikowska et al. 2016); the latter is the most frequent plant in the chalk soil at the studied microsite (Lövy et al. 2015). In other words, these bitter compounds or other compounds with similar chemical structures occur in the daily food of mole rats living in the two soils. Under such selective pressures, Tas2rs of the mole rats are likely locally adapted.

Why do the mole rats from different soils possess distinct capacity to detect bitter substances? We speculate that the basalt soil may have a larger abundance of food sources but may also have a higher proportion of toxic plants, such as the predominant plant *Ornithogalum lanceolatum* (comprising 28% of all underground storage organs of plants in the basalt soil) (Lövy et al. 2015). The bulbs of *Ornithogalum* species are poisonous because they contain a variety of cardiotoxic cardenolides (Burrows and Tyrl 2012). Thus, animals in the basalt soil tend to have more food to eat but have evolved a keen sense of bitter taste to deal with the higher chance of encountering toxins. By contrast, the proportion of *Ornithogalum lanceolatum* among all underground storage organs of plants in the chalk soil is very low (~2%) (Lövy et al. 2015). As a result, chalk soil may offer fewer types of food sources that might be less toxic. This scenario suggests that

adaptation of bitter taste could have effectively hindered migration between the two populations: basalt animals avoid migration to chalk soil because of the scarcity of food supply, whereas chalk animals avoid migration to basalt soil as they would be toxified due to their dull bitter taste. We propose a potential tradeoff between the two populations: more food and more toxin versus less food and less toxin. Given the role of taste adaptation in hindering migration between the two populations, we speculate that local adaptation of taste receptors should be a cause of incipient speciation. Although it is a matter of speculation, it would be interesting to test this scenario in the future. In addition, our study reinforces the recent discovery that bitter taste receptors of a small rodent were locally adapted to a desert condition where food resources are limited (Tigano et al. 2020).

Taken together, we found that functional divergence of bitter taste receptors may have played a major role in food selection during the process of ecological speciation of *S. galili*. Divergent selection could arise from the difference in food resources between the two soils, which then drives local adaptation of bitter taste receptors. The keen sense of bitter taste provides a physiological basis for the mole rats living in the basalt soil to obtain food with less toxic compounds, whereas the dull bitter taste helps mole rats in the chalk soil to compromise the bitter compounds in their foods. Local adaptation of bitter taste can lead to food choice and habitat preference, such that mole rats preferring to reside in the soil to which they are adapted will have higher fitness (Rundle and Nosil 2005). The subsequent barriers to gene flow and prezygotic isolation would evolve between the two populations due to habitat-based assortative mating (Lövy et al. 2017, 2020), which may lead to premating reproductive isolation.

Limitations

There are two limitations to this work. First, our collection of bitter compounds (ten natural and ten synthetic) used in the cell-based assay is quite small. Although the ten natural compounds include several bitter substances commonly used for chemical defense in plants, they cannot reflect the real composition of bitter substances present in the daily food of the mole rat. Thus, some of Tas2r functional divergence we detected here may not be relevant to the difference of dietary ecology between the two soils. Second, our study only focused on genetic and functional analysis of bitter taste receptors, proposing a hypothesis that taste may play an important role in ecological speciation. We are not able to conduct physiological and behavioral experiments on mole rats. It would be interesting to extract bitter compounds from plants growing in the two soils, and test these compounds in cell-based assays and behavioral experiments in the future. These measurements could provide direct evidence linking the bitter taste sensitivity to food choice by the mole rats.

Conclusions

This study used population genetic analysis and functional experiments to provide clear evidence of local adaptation of

bitter taste receptor genes in two populations of *S. galili* inhabiting contrasting soil environments. We found that basalt-type bitter receptors showed higher response intensity and sensitivity compared with chalk-type receptors. Hence, it is likely that the new and rich habitat of basalt, which includes many geophytes with bitter bulbs and corms, selected for higher bitterness, leading to local adaptation of bitter taste. Our study shows divergent selection on food resources through local adaptation of bitter receptors, and suggests a role of taste that has been underappreciated in speciation.

Materials and Methods

Identification and Nomenclature of *Tas2r* Genes

We downloaded the genome sequence of the blind mole rat *Spalax galili* (GenBank assembly: GCF_000622305.1) (Fang et al. 2014) and performed TblastN searches (Altschul et al. 1990) to identify *Tas2r* genes using protein sequences of known rodent *Tas2rs* as queries. A total of 32 *Tas2r* genes were found to possess an intact open reading frame longer than 270 amino acids in length and were considered putatively functional. The nucleotide sequences of these intact *Tas2rs* are provided in [supplementary data S1, Supplementary Material](#) online. We followed the nomenclature of *Tas2rs* proposed in Euarthontoglires (Hayakawa et al. 2014). Specifically, we first constructed a gene tree ([supplementary fig. S1, Supplementary Material](#) online) using IQ-TREE with 1,000 bootstrap replicates (Nguyen et al. 2015) based on the alignment of nucleotide sequences of the 32 *Tas2rs* identified here, along with all intact rodent *Tas2rs* identified in a previous study (Hayakawa et al. 2014). We next used “Sg_*Tas2rx*” to denote the bitter taste receptor genes in *S. galili* ($102 \leq x \leq 146$ in orthologs between mouse and *S. galili*; $200 < x < 300$ in the ancestral orthologs of rodents that are not defined in mouse; $500 < x < 600$ in rodent-specific orthologs).

DNA Sequencing

We sequenced all 32 *Tas2rs* from 29 individuals of *S. galili*, including 16 sampled from the basalt soil and 13 sampled from the chalk soil. Of these 32 *Tas2rs*, 20 have been reported in our previous study (Li et al. 2015). Genomic DNAs were isolated from the muscle tissues that were stored at -20°C , using a DNeasy Blood and Tissue Kit (Qiagen). Primers were designed based on the genome sequence of the blind mole rat ([supplementary table S8, Supplementary Material](#) online). The details of polymerase chain reactions and subsequent sequencing were described previously (Li et al. 2015; Jiao et al. 2019).

Population Genetic Analysis

Fixation index (F_{ST}) was used to measure the genetic differentiation between the basalt and chalk populations for each *Tas2r* gene (Weir and Cockerham 1984), and the nearest-neighbor statistical test (Hudson 2000) was conducted to evaluate the significance of this genetic differentiation. Using PHASE v2.1 software, the protein haplotypes for each

Tas2r gene were inferred with a Bayesian statistical method (Stephens and Donnelly 2003).

Bitter Compounds

Our bitter compound library includes ten naturally occurring and ten synthetic compounds ([supplementary table S5, Supplementary Material](#) online). All examined compounds were purchased from Sigma–Aldrich, except for diphenidol hydrochloride (Reagent World). These compounds were dissolved in Dulbecco’s phosphate-buffered saline (DPBS) or dimethyl sulphoxide (DMSO) and then diluted with DPBS to prepare the tested solutions. Given the high toxicity of DMSO to the transfected cells, the final DMSO concentration in the tested solutions must be less than 0.1%. The highest concentrations of bitter compounds were obtained from a previous study (Meyerhof et al. 2010).

Preparation of *Spalax Tas2r* Constructs and Site-Directed Mutants

The complete coding sequences of three *Spalax Tas2r* genes were amplified from genomic DNA, and then subcloned into pEAK10 vector, with the first 45 amino acid residues of rat somatostatin receptor 3 as the signal peptide at the N-terminal. Point mutations in *Tas2r118* were introduced by site-directed mutagenesis, using the QuikChange method (Agilent Technologies, La Jolla, CA). All constructs were verified by Sanger sequencing.

Functional Assays of *Spalax Tas2rs*

Human embryonic kidney 293 (HEK293) cells (PEAKrapid) were obtained from ATCC (CRL-2828) and cultured in Opti-MEM medium with 6% fetal bovine serum. The cells were seeded in 96-well plates coated with poly-L-lysine, at a density of 40,000–50,000 per well. After 20–22 h, cells were transiently transfected with a *Tas2r* construct (0.1 $\mu\text{g}/\text{well}$) along with a coupling chimeric G protein $G\alpha_{16}\text{-gust44}$ (0.1 $\mu\text{g}/\text{well}$) using Lipofectamine 2000 (0.5 $\mu\text{l}/\text{well}$). Cells that were transfected with only $G\alpha_{16}\text{-gust44}$ were used as negative controls (mock transfection). After transfection for one day, the cells were washed once with DPBS and loaded with the calcium-sensitive dye Fluo-4 AM for 1 h in the dark. After three washes with DPBS, the cells were assayed in a FlexStation III reader (Molecular Devices) to monitor the fluorescence changes every 2 s for 2 min. Calcium mobilization traces were recorded. Changes in fluorescence (ΔF) were quantified as the peak fluorescence minus baseline fluorescence. The percentage of ΔF relative to baseline (F) averaged from triplicate experiments was used to quantify the calcium mobilization. Calcium mobilization traces, bar graphs, and dose-dependent curves were generated with GraphPad Prism 5.

Immunofluorescence Assays

HEK293 (PEAKrapid) cells were seeded onto poly-lysine coated coverslips in 12-well plates and transfected with a *Tas2r* construct (1 $\mu\text{g}/\text{well}$ for each construct), along with $G\alpha_{16}\text{-gust44}$ (1 $\mu\text{g}/\text{well}$) by Lipofectamine (4 $\mu\text{l}/\text{well}$). After 24 h of transfection, cells were washed twice with warm

phosphate-buffered saline (PBS) and placed at 4 °C for 2 h. The cell surface staining was performed by incubation with concanavalin A, Alexa Fluor 633 Conjugate (C21402, Thermo Fisher, 1:5) for 1 h, followed by three rinses with ice cold PBS buffer. The cells were then fixed by 4% paraformaldehyde in PBS for 20 min. Cells were washed three times with PBS and incubated with 0.1% Triton X-100 in PBS for 10 min. After washed with PBS, cells were incubated for 1 h in 10% fetal bovine serum in PBS to block unspecific binding. Next, an anti-HSV antibody (ab19355, Abcam, 1:500) in PBS supplemented with 10% fetal bovine serum was applied overnight at 4 °C. A donkey anti-rabbit secondary antibody conjugated with Alexa Fluor 488 (ANT024, Wuhan antgene Biotechnology, 1:1,000) was then used for detection of the HSV tag. The nucleus was stained with 4',6-diamidino-2-phenylindole (DAPI). Images were captured with confocal laser scanning microscopy (Leica TCS SP8). To evaluate the expression level of Tas2r in HEK293 cells, three independent areas were counted.

Structure Modeling and Molecular Docking

The 3D structures of bitter taste receptors were obtained by GPCR-I-TASSER (Zhang et al. 2015). The model with the highest C-score was used in subsequent docking analysis. Different bitter tastants were docked with the corresponding receptors using Autodock Vina (Trott and Olson 2010). The interactions in receptor–ligand complexes were characterized using PLIP (Salentin et al. 2015).

Supplementary Material

Supplementary data are available at *Molecular Biology and Evolution* online.

Acknowledgments

The authors thank Yi Wang, Wei Hong, and Xin Zheng for technical assistance in the laboratory, and Yasuka Toda for providing the plasmid pEAK10. This work was supported by National Natural Science Foundation of China (31722051 and 31672272 to H.Z. and 32000385 to H.J.), Natural Science Foundation of Hubei Province (2019CFA075 to H.Z.), China Postdoctoral Science Foundation (2020M672407 to H.J.), China National Postdoctoral Program for Innovative Talents (BX20200255 to H.J.) and Hubei Provincial Postdoctoral Foundation (to H.J.), and by the National Institute on Deafness and Other Communication Disorders at the National Institutes of Health (R01DC010842 to P.J.). Additionally, E.N. thanks the Ansell-Teichert Research Foundation for Genetic and Molecular Evolution for financial support in the study of *Spalax galili*.

Author Contributions

H.Z. conceived and designed the research. H.J. performed the sequencing work and population genetic analysis. H.J., Q.W., Q.L., and W.S. conducted the functional assays. P.J. supervised the functional assays and commented the manuscript. B.-J.W. performed structure modeling and molecular docking. H.J. and Q.W. analyzed the data. M.L. provided the photographs

of studied microsites and commented the manuscript. K.L. and E.N. provided the samples and edited the manuscript. H.J. and H.Z. wrote the manuscript with input from all authors.

Data Availability

All sequences that were newly generated in this article have been deposited in the GenBank (accession numbers: MN750256–MN750313 and MN815131–MN815768).

References

- Altschul SF, Gish W, Miller W, Myers EW, Lipman DJ. 1990. Basic local alignment search tool. *J Mol Biol.* 215(3):403–410.
- Berner D, Thibert-Plante X. 2015. How mechanisms of habitat preference evolve and promote divergence with gene flow. *J Evol Biol.* 28(9):1641–1655.
- Brand P, Ramirez SR, Leese F, Quezada-Euan JG, Tollrian R, Eltz T. 2015. Rapid evolution of chemosensory receptor genes in a pair of sibling species of orchid bees (Apidae: Euglossini). *BMC Evol Biol.* 15(1):176.
- Burrows GE, Tyrl RJ. 2012. Toxic plants of North America. 8th ed. Chichester, UK: John Wiley & Sons.
- Darwin C. 1859. On the origin of species by means of natural selection, or the preservation of favored races in the struggle for life. London: John Murray.
- Fang X, Nevo E, Han LJ, Levanon EY, Zhao J, Avivi A, Larkin D, Jiang XT, Feranchuk S, Zhu YB, et al. 2014. Genome-wide adaptive complexes to underground stresses in blind mole rats *Spalax*. *Nat Commun.* 5:3966.
- Hadid Y, Tzur S, Pavlicek T, Sumbera R, Skliba J, Lovy M, Fragman-Sapir O, Beiles A, Arieli R, Raz S, et al. 2013. Possible incipient sympatric ecological speciation in blind mole rats (*Spalax*). *Proc Natl Acad Sci U S A.* 110(7):2587–2592.
- Hayakawa T, Sugawara T, Go Y, Udono T, Hirai H, Imai H. 2012. Ecogeographical diversification of bitter taste receptor genes (*TAS2Rs*) among subspecies of chimpanzees (*Pan troglodytes*). *PLoS One* 7(8):e43277.
- Hayakawa T, Suzuki-Hashido N, Matsui A, Go Y. 2014. Frequent expansions of the bitter taste receptor gene repertoire during evolution of mammals in the Euarchontoglires clade. *Mol Biol Evol.* 31(8):2018–2031.
- Hu X, Wang G, Shan L, Sun S, Hu Y, Wei F. 2020. *TAS2R20* variants confer dietary adaptation to high-quercitrin bamboo leaves in Qinling giant pandas. *Ecol Evol.* 10(12):5913–5921.
- Hudson RR. 2000. A new statistic for detecting genetic differentiation. *Genetics* 155(4):2011–2014.
- Imai H, Suzuki N, Ishimaru Y, Sakurai T, Yin LJ, Pan WS, Abe K, Misaka T, Hirai H. 2012. Functional diversity of bitter taste receptor *TAS2R16* in primates. *Biol Lett.* 8(4):652–656.
- Jiao H, Hong W, Nevo E, Li K, Zhao H. 2019. Convergent reduction of *V1R* genes in subterranean rodents. *BMC Evol Biol.* 19(1):176.
- Jiao H, Wang Y, Zhang L, Jiang P, Zhao H. 2018. Lineage-specific duplication and adaptive evolution of bitter taste receptor genes in bats. *Mol Ecol.* 27(22):4475–4488.
- Keesey IW, Grabe V, Knaden M, Hansson BS. 2020. Divergent sensory investment mirrors potential speciation via niche partitioning across *Drosophila*. *eLife* 9:e57008.
- Kikowska M, Dworacka M, Kędziora I, Thiem B. 2016. *Eryngium creticum* – ethnopharmacology, phytochemistry and pharmacological activity. A review. *Rev Bras Farmacogn.* 26(3):392–399.
- Kingston T, Rossiter SJ. 2004. Harmonic-hopping in Wallacea's bats. *Nature* 429(6992):654–657.
- Kopp M, Servedio MR, Mendelson TC, Safran RJ, Rodriguez RL, Hauber ME, Scordato EC, Symes LB, Balakrishnan CN, Zonana DM, et al. 2018. Mechanisms of assortative mating in speciation with gene flow: connecting theory and empirical research. *Am Nat.* 191(1):1–20.

- Li D, Zhang J. 2014. Diet shapes the evolution of the vertebrate bitter taste receptor gene repertoire. *Mol Biol Evol.* 31(2):303–309.
- Li K, Hong W, Jiao H, Wang GD, Rodriguez KA, Buffenstein R, Zhao Y, Nevo E, Zhao H. 2015. Sympatric speciation revealed by genome-wide divergence in the blind mole rat *Spalax*. *Proc Natl Acad Sci U S A.* 112(38):11905–11910.
- Li K, Wang L, Knisbacher BA, Xu QQ, Levanon EY, Wang HH, Frenkel-Morgenstern M, Tagore S, Fang XD, Bazak L, et al. 2016. Transcriptome, genetic editing, and microRNA divergence substantiate sympatric speciation of blind mole rat, *Spalax*. *Proc Natl Acad Sci U S A.* 113(27):7584–7589.
- Librado P, Rozas J. 2009. DnaSP v5: a software for comprehensive analysis of DNA polymorphism data. *Bioinformatics* 25(11):1451–1452.
- Lövy M, Šklíba J, Hrouzková E, Dvořáková V, Nevo E, Šumbera R. 2015. Habitat and burrow system characteristics of the blind mole rat *Spalax galili* in an area of supposed sympatric speciation. *PLoS One* 10(7):e0133157.
- Lövy M, Šklíba J, Šumbera R, Nevo E. 2017. Soil preference in blind mole rats in an area of supposed sympatric speciation: do they choose the fertile or the familiar? *J Zool.* 303(4):291–300.
- Lövy M, Šumbera R, Heth G, Nevo E. 2020. Presumed ecological speciation in blind mole rats: does soil type influence mate preferences? *Ethol Ecol Evol.* 32(1):46–59.
- Mayr E. 1947. Ecological factors in speciation. *Evolution* 1(4):263–288.
- McBride CS. 2007. Rapid evolution of smell and taste receptor genes during host specialization in *Drosophila sechellia*. *Proc Natl Acad Sci U S A.* 104(12):4996–5001.
- Meyerhof W, Batram C, Kuhn C, Brockhoff A, Chudoba E, Bufé B, Appendino G, Behrens M. 2010. The molecular receptive ranges of human TAS2R bitter taste receptors. *Chem Senses.* 35(2):157–170.
- Mohammad AG, Alseekh SH. 2013. The effect of *Sarcopoterium spinosum* on soil and vegetation characteristics. *CATENA* 100:10–14.
- Nguyen LT, Schmidt HA, von Haeseler A, Minh BQ. 2015. IQ-TREE: a fast and effective stochastic algorithm for estimating maximum-likelihood phylogenies. *Mol Biol Evol.* 32(1):268–274.
- Niimura Y, Nei M. 2006. Evolutionary dynamics of olfactory and other chemosensory receptor genes in vertebrates. *J Hum Genet.* 51(6):505–517.
- Rundle HD, Nosil P. 2005. Ecological speciation. *Ecol Lett.* 8(3):336–352.
- Salentin S, Schreiber S, Haupt VJ, Adasme MF, Schroeder M. 2015. PLIP: fully automated protein-ligand interaction profiler. *Nucleic Acids Res.* 43(W1):W443–W447.
- Schluter D. 2001. Ecology and the origin of species. *Trends Ecol Evol.* 16(7):372–380.
- Schluter D. 2009. Evidence for ecological speciation and its alternative. *Science* 323(5915):737–741.
- Schluter D, Conte GL. 2009. Genetics and ecological speciation. *Proc Natl Acad Sci U S A.* 106(Suppl 1):9955–9962.
- Seehausen O, Terai Y, Magalhaes IS, Carleton KL, Mrosso HDJ, Miyagi R, van der Sluijs I, Schneider MV, Maan ME, Tachida H, Imai H, et al. 2008. Speciation through sensory drive in cichlid fish. *Nature* 455(7213):620–626.
- Singh N, Pydi SP, Upadhyaya J, Chelikani P. 2011. Structural basis of activation of bitter taste receptor T2R1 and comparison with class A G-protein-coupled receptors (GPCRs). *J Biol Chem.* 286(41):36032–36041.
- Sobel JM, Chen GF, Watt LR, Schemske DW. 2010. The biology of speciation. *Evolution* 64(2):295–315.
- Stephens M, Donnelly P. 2003. A comparison of Bayesian methods for haplotype reconstruction from population genotype data. *Am J Hum Genet.* 73(5):1162–1169.
- Sugawara T, Go Y, Udono T, Morimura N, Tomonaga M, Hirai H, Imai H. 2011. Diversification of bitter taste receptor gene family in western chimpanzees. *Mol Biol Evol.* 28(2):921–931.
- Thomas A, Sulli C, Davidson E, Berdougou E, Phillips M, Puffer BA, Paes C, Doranz BJ, Rucker JB. 2017. The bitter taste receptor TAS2R16 achieves high specificity and accommodates diverse glycoside ligands by using a two-faced binding pocket. *Sci Rep.* 7(1):7753.
- Tigano A, Colella JP, MacManes MD. 2020. Comparative and population genomics approaches reveal the basis of adaptation to deserts in a small rodent. *Mol Ecol.* 29(7):1300–1314.
- Toki K, Takeuchi M, Saito N, Honda T. 1996. Two malonylated anthocyanidin glycosides in *Ranunculus asiaticus*. *Phytochemistry* 42(4):1055–1057.
- Trott O, Olson AJ. 2010. AutoDock Vina: improving the speed and accuracy of docking with a new scoring function, efficient optimization, and multithreading. *J Comput Chem.* 31(2):455–461.
- Tsutsui K, Otoh M, Sakurai K, Suzuki-Hashido N, Hayakawa T, Misaka T, Ishimaru Y, Aureli F, Melin AD, Kawamura S, et al. 2016. Variation in ligand responses of the bitter taste receptors TAS2R1 and TAS2R4 among New World monkeys. *BMC Evol Biol.* 16(1):208.
- Wang K, Zhao H. 2015. Birds generally carry a small repertoire of bitter taste receptor genes. *Genome Biol Evol.* 7(9):2705–2715.
- Weinstein Y, Navon O, Altherr R, Stein M. 2006. The role of lithospheric mantle heterogeneity in the generation of Plio-Pleistocene alkali basaltic suites from NW Harrat Ash Shaam (Israel). *J Petrol.* 47(5):1017–1050.
- Weir BS, Cockerham CC. 1984. Estimating F-statistics for the analysis of population structure. *Evolution* 38(6):1358–1370.
- Yang Z. 2007. PAML 4: Phylogenetic analysis by maximum likelihood. *Mol Biol Evol.* 24(8):1586–1591.
- Zhang J, Yang JY, Jang R, Zhang Y. 2015. GPCR-I-TASSER: a hybrid approach to G protein-coupled receptor structure modeling and the application to the human genome. *Structure* 23(8):1538–1549.